Science and Technology Indonesia
e-ISSN:2580-4391 *p*-ISSN:2580-4405
Vol. 11, No. 1, January 2026

Research Paper

Enhanced Piperine Solubility and Dissolution Rate in Piperine-Nicotinamide Multicomponent Crystal Adsorbed in Mesoporous Silica SBA-15

Lili Fitriani[1], Gusrina Fauziah[1], Uswatul Hasanah[1], Rini Agustin[1], Erizal Zaini[1*]

[1]*Department of Pharmaceutics, Faculty of Pharmacy, Universitas Andalas, Padang, 25163, Indonesia*
***Corresponding author**: erizal@phar.unand.ac.id

Abstract
Piperine, classified as a Class II substance in the Biopharmaceutics Classification System (BCS), has poor solubility in water but high permeability. This research aims to improve the solubility and dissolution rate of piperine by adsorbing a multicomponent crystal (MCC) of piperine-nicotinamide onto mesoporous silica SBA-15. Tetraethyl orthosilicate (TEOS) was used as a silica precursor and Pluronic P123 as a pore-formation template to create SBA-15. Adsorption of the MCC was carried out by solvent evaporation with MCC:SBA-15 mass ratio (1:1). Solid state characterization was carried out by nitrogen adsorption-desorption isotherm, X-ray powder diffraction (XRPD), differential scanning calorimetry (DSC), Fourier-transform infrared (FT-IR) spectroscopy, and scanning electron microscopy (SEM). Solubility tests were carried out for 24 hours and the dissolution rate profile was conducted for 60 minutes in distilled water. Dissolved piperine was determined using high performance liquid chromatography (HPLC) with methanol and distilled water as the mobile phase (75:25). The physical stability of MCC:SBA-15 was evaluated at various high relative humidities. The solid-state characterization results showed successful adsorption of the MCC in SBA-15 with a decrease in surface area, pore volume, and intensity of the X-ray diffraction peaks. The FT-IR spectrum of MCC:SBA-15 resembled that of SBA-15. The solubility test results showed 2.47-fold and 3.07-fold increases in solubility and dissolution rate compared to pure piperine, respectively. MCC:SBA-15 demonstrated high stability at 75% and 85% RH at 40°C. In conclusion, adsorption of the MCC piperine-nicotinamide crystal in mesoporous silica SBA-15 can enhance the solubility and dissolution rate of piperine.

Keywords
Piperine, Mesoporous SBA-15, Nicotinamide, Solubility, Dissolution Rate

Received: 5 August 2025, Accepted: 23 October 2025
https://doi.org/10.26554/sti.2026.11.1.109-120

1. INTRODUCTION

Piperine is a bioactive metabolite in plants of the Piperaceae family and particularly relevant in *Piper nigrum* L., which is widely applied in traditional medicines. Various studies related to the bioactivity of piperine have documented its broad pharmacological effects, including anti-inflammatory, analgesic, antioxidant, antimicrobe, antidiabetic, and antitumor (Haq et al., 2021). Unfortunately, piperine has low solubility in water (0.04 mg/mL at 18°C), limiting its wider clinical application (Kusumorini et al., 2022). Piperine is categorized as a Class II compound in the Biopharmaceutical Classification System (BCS) because of its poor solubility in water and high permeability (Charalabidis et al., 2019). Poor water solubility and dissolution of poorly water-soluble drugs in gastrointestinal fluids often lead to suboptimal bioavailability. Conversely, enhancing the solubility and dissolution rate of these drugs can improve their bioavailability (Kusumorini et al., 2022).

Several methods have been utilized to improve either the solubility or dissolution of piperine, including solid dispersion using the spray and freeze drying method (Fitriani et al., 2024b; Zaini et al., 2021), inclusion complexes with β-cyclodextrin (Quilaqueo et al., 2019), nanosuspension (Zaini et al., 2019), formation of a solid dispersion by extrusion method (Wdowiak et al., 2023), and formulation self-emulsifying drug delivery system (SEDDS) (Zafar et al., 2021). While these strategies have demonstrated improvements in the solubility and / or dissolution of piperine, inherent limitations continue to restrict their overall effectiveness. Commercial use of solid dispersions is very limited, mainly due to difficulties in the manufacturing process and poor physical stability (Nair et al., 2020). Drug stability and particle size uniformity are difficult to control in nanosuspensions (Chakravorty, 2022). The potential of SEDDS to retain piperine in dissolved form is predominantly determined by the solubility of the drug in oil instead of water (Buya et al., 2020).

A technique recently explored to increase solubility and

dissolution of active substances involves modifying their crystallinity by preparing multicomponent crystals with suitable coformers (Lutfiyah et al., 2022). Nicotinamide has been utilized as a coformer in the preparation of cocrystals to enhance the solubility of various active pharmaceutical ingredients (APIs) because of its high water solubility and safety (Júnior et al., 2020; Yadav et al., 2022). Additionally, mesoporous silica has been widely applied as a carrier to increase the solubility and dissolution rate of low solubility active substances (Patel et al., 2021). The material has a very regular meso-structure with a pore size distribution in the range 2-50 nm and a high surface area (700-1000 m^2/g) and pore volume (0.6-1 cm^2/g), allowing the diffusion and adsorption of larger molecules (Chaudhary and Sharma, 2017). A specific mesoporous silica that has shown the ability to increase the solubility of active substances is SBA-15, which can be synthesized using Pluronic P123 as the template. SBA-15 mesoporous silica is preferred over other mesoporous materials due to its ease of synthesis over a wide temperature range (35-130°C) using either tetraethyl orthosilicate (TEOS) or the more cost-effective sodium silicate. It also offers tunable and larger pore sizes, typically around 10 nm compared to 4 nm in MCM-41, as well as thicker pore walls that provide improved hydrothermal stability. In addition, SBA-15 exhibits diverse morphologies depending on synthesis conditions and possesses a high specific surface area and pore volume, with well-ordered mesopores that facilitate the diffusion and adsorption of larger molecules (Chaudhary and Sharma, 2017; Jaramillo et al., 2020; Sayyidina et al., 2025; Thahir et al., 2019). Moreover, research has shown that compression at higher pressures (160 and 260 MPa) does not result in the complete destruction of the organized pore structure of SBA-15 (Springuel-Huet et al., 2001). The previous studies have shown the ability of mesoporous SBA-15 in enhancing the solubility of usnic acid and ticagrelor (Fitriani et al., 2024a; Hasanah et al., 2025).

A promising strategy to increase the solubility and rate of dissolution of poorly soluble active pharmaceutical ingredients (APIs) is the combination of SBA-15 and multicomponent crystals. Therefore, this current study aim to prepare multicomponent crystal piperine/nicotinamide (MCC)-loaded mesoporous silica to improve the solubility and dissolution rate of piperine. Following the nitrogen adsorption-desorption isotherm, a number of solid state property characterizations were performed on the MCC:SBA-15 samples. The solubility and dissolution test was carried out to confirm the influence of mesoporous in enhancing both parameters. Moreover, the drug-loaded SBA-15 samples were further evaluated for physical stability at various high relative humidities (RH).

2. EXPERIMENTAL SECTION

2.1 Materials

Piperine (BOC Science, USA), nicotinamide (Sigma Aldrich, USA), Pluronic P 123 ($[HO(CH_2CH_2O)_{20}(CH_2CH(CH_3)O)_{70}(CH_2CHO)_{20}H]$) (Sigma Aldrich, USA), TEOS (tetraethyl orthosilicate) (Tokyo Chemical Industry, Japan), HPLC grade methanol and ethanol pro analysis (Merck, Germany), HCl, NaCl, and distilled water (Ikapharmindo, Jakarta).

2.2 Instrumentation

Powder X-ray diffractometer (PXRD, PAN analytical MPD PW3040/60 type 100, Netherlands), thermal apparatus (Shimadzu DSC-60 Plus, Japan), infra-red spectrophotometer (Shimadzu, Japan), SEM apparatus (Hitachi Flexsem 100, Japan), HPLC with a DAD UV-vis detector (Shimadzu AUX 220, Japan).

2.3 Methods

2.3.1 Preparation of Piperine/Nicotinamide Multicomponent Crystal (MCC)

Solvent drop grinding was used to prepare the multicomponent crystals. Piperine and nicotinamide in equal molar ratio (1:1) were ground constantly for 10 minutes with 100 μL of ethanol. The powders obtained were stored in a desiccator (Octavia et al., 2023).

2.3.2 Preparation of Mesoporous Silica SBA-15

SBA-15 was synthesised by preparing TEOS/HCl/H_2O/P123 in a 1:6:166:0.02 molar ratio. After dissolving pluronic P123 and 6 M NaCl in 2 M HCl, the mixture was magnetically stirred for 24 hours at room temperature at 300 rpm. After adding TEOS, stirring continued for three hours at 700 rpm. The resultant mixture was incubated for 24 hours at 80°C in an oven (Memmert, Germany). The formed solid was collected by filtration with Whatman paper, washed with distilled water, and dried overnight at 50°C. Finally, calcination was carried out to remove surfactants at a temperature of 550°C for 4 h to obtain SBA-15 powder (Fitriani et al., 2022).

2.3.3 Adsorption of Piperine and Piperine/Nicotinamide MCC in Mesoporous Silica SBA-15

Experiments were carried out using mixtures in a 1:1 weight ratio of piperine:SBA-15 and MCC:SBA-15. Piperine or MCC were dissolved in 10 mL of pro analysis ethanol in a beaker glass and then SBA-15 was added. The mixture was magnetically stirred at 80°C and 300 rpm until the solvent was fully evaporated, providing piperine:SBA-15 or MCC:SBA-15 powders (Fitriani et al., 2022).

2.3.4 Nitrogen Adsorption-Desorption Isotherm Analysis

Using the N_2 adsorption-desorption isotherm at 77 K and the multipoint Brunauer-Emmet-Teller (BET) method with a gas sorption analyzer (Quantachrome Novatouch LX-4, USA), the specific surface area of SBA-15, piperine:SBA-15, and MCC:SBA-15 was determined. The P/Po value and BET transformation value [1/W(P/Po)] were then obtained for area calculations (Fitriani et al., 2022).

2.3.5 Solid-State Characterisations

The solid state analysis of samples (piperine, nicotinamide, piperine/nicotinamide multicomponent crystal, SBA-15, and

MCC:SBA-15) were conducted by using powder X-Ray Diffraction at 2θ = 5° to 40° (metal target, Cu; filter, Kα; voltage 45 kV; and current, 40 mA), Differential Scanning Calorimetry (DSC) at temperature of 50 to 250°C at 10°C/minute Fourier-Transform Infrared (FT-IR) Spectroscopy at the wavenumber range 4000-400 cm^{-1} by dispersing the sample onto an ATR crystal, Scanning Electron Microscope (SEM) at 20 kV and 12 mA (Zaini et al., 2020b).

2.3.6 Entrapment Efficiency Calculation

Piperine:SBA-15 and MCC:SBA-15 (1:1, or 10 mg piperine) dissolved in 100 mL of ethanol pro analysis and filtered through a 0.22 μm nylon filter were tested for entrapment efficiency. The amount of piperine entrapped in piperine:SBA-15 and MCC:SBA-15 was determined using HPLC with a DAD UV-vis detector (Shimadzu AUX 220, Japan) with a mobile phase of methanol:distilled water (75:25) and stationary phase octadecylsilane (C18). Analyses were carried out in triplicate (Fitriani et al., 2024b).

2.3.7 Solubility Test

Solubility tests for piperine in the multicomponent crystal, piperine:SBA-15, and MCC:SBA-15 were carried out by weighing samples corresponding to an excess of piperine, dissolving in 100 mL distilled water for 24 h using an orbital shaker at room temperature. After filtering the mixtures through a 0.45 μm Whatman filter, the filtrates were analysed by HPLC (Shimadzu AUX 220, Japan) as described in the entrapment efficiency section. Analyses were carried out in triplicate (Fitriani et al., 2024b).

2.3.8 Dissolution Test

Dissolution tests for piperine, multicomponent crystal, piperine :SBA-15, and MCC:SBA-15 were carried out for samples equivalent to 10 mg piperine using a paddle type (type II) dissolution test (SR08 Plus Dissolution Test Station Hanson, USA). The dissolution flask was filled with 900 mL distilled water at 37 ± 0.5°C and 50 rpm stirring speed. The amount of piperine dissolved was measured at 5, 10, 15, 30, 45, and 60 minutes, filtering each sample using a 0.45 μm Whatman filter prior to measurement by HPLC (Shimadzu AUX 220, Japan) (Zaini et al., 2020a). Analyses were carried out in triplicate.

2.3.9 Stability Tests

Piperine:SBA-15 and MCC:SBA-15 samples were subjected to stability tests after being kept in a climatic chamber (Memmert HPP 10, Germany) for two weeks at relative humidities (RH) of 75, 85, and 95% at 40°C. Physical changes (crystallinity and phase transitions) were evaluated with a PXRD instrument (Zaini et al., 2019).

2.3.10 Statistical Analysis

A one-way ANOVA with a significance level of $p < 0.05$ was used to statistically analyze the mean ± SD data from the entrapment efficiency calculation, solubility test, and dissolution test.

3. RESULTS AND DISCUSSION

Nitrogen adsorption-desorption isotherm analysis is utilized to assess a material's surface attributes by measuring its specific surface area, pore diameter, and pore volume (Thommes and Cychosz, 2014). As seen in Figure 1, the pores formed are mesopores in the range of 2-50 nm and the type IV isotherm curve is characteristic for mesoporous materials, presenting an H1 hysteresis loop at a relative pressure of 0.4-0.8. In Figure 1a, the hysteresis loop H1 shows a sharp adsorption curve related to capillary condensation in the SBA-15 pores. In the relative pressure range of 0-0.05, there is an increase which tends to stabilise in the adsorbed volume caused by the formation of a single layer and conversion into a multilayer. Capillary condensation, indicated by a sharp increase in adsorption, occurs in the relative pressure range of 0.6-0.7. This shows that SBA-15 has a regular nanoporous structure. Above a relative pressure of 0.7, no more N_2 is adsorbed because the pores are saturated. Hysteresis loops are formed when capillary condensation occurs on the surface of the pore wall membrane and then desorption begins from depressions in the multilayer (Jangra et al., 2016).

In the isotherm curves resulting from the nitrogen adsorption of piperine:SBA-15 and MCC:SBA-15 shown in Figures 1b-c, the desorption curve does not return to the adsorption curve. For some mesoporous materials, distinct adsorption and desorption can be observed in relatively low-pressure regions. This can be caused by chemical adsorption that occurs in the material during measurement. Moreover, water that is chemically adsorbed on the silica surface during the adsorption process likely also influences this phenomenon (Van Der Meer et al., 2010).

Based on the results in Table 1, pure SBA-15 has a greater surface area, pore volume, and pore size than SBA-15 loaded with piperine or the multicomponent crystal. After loading, the surface area and pore characteristics diminish, consistent with a study showing filled pore channels in SBA-15 (Jangra et al., 2016). In addition, the decrease in the value of each parameter is related to the shrinkage of the hexagonal structure and the closure of mesopores after piperine or multicomponent crystal adsorption (Biswas, 2017).

PXRD analysis is a method for identifying the solid properties, including crystalline and amorphous phases. The results are shown in Figure 2 and Table 2.

The diffractogram in Figure 2 shows a wide peak for pure SBA-15, which confirms that it is in the amorphous phase (Dadej et al., 2022). Meanwhile, piperine and nicotinamide are crystalline, characterised by distinctive and sharp peaks. The specific diffraction peaks for piperine are 2θ 14.82°, 22.59°, 25.89°°, and 28.28°, while those for nicotinamide are 15.08°, 26.07°, and 27.56°. The diffractogram of the piperine/nicotinamide multicomponent crystal does not show new diffraction peaks, implying that no new crystalline phase was formed, but there is a decrease in peak intensity. This multicomponent crystal forms a eutectic mixture, a conglomeration or combina-

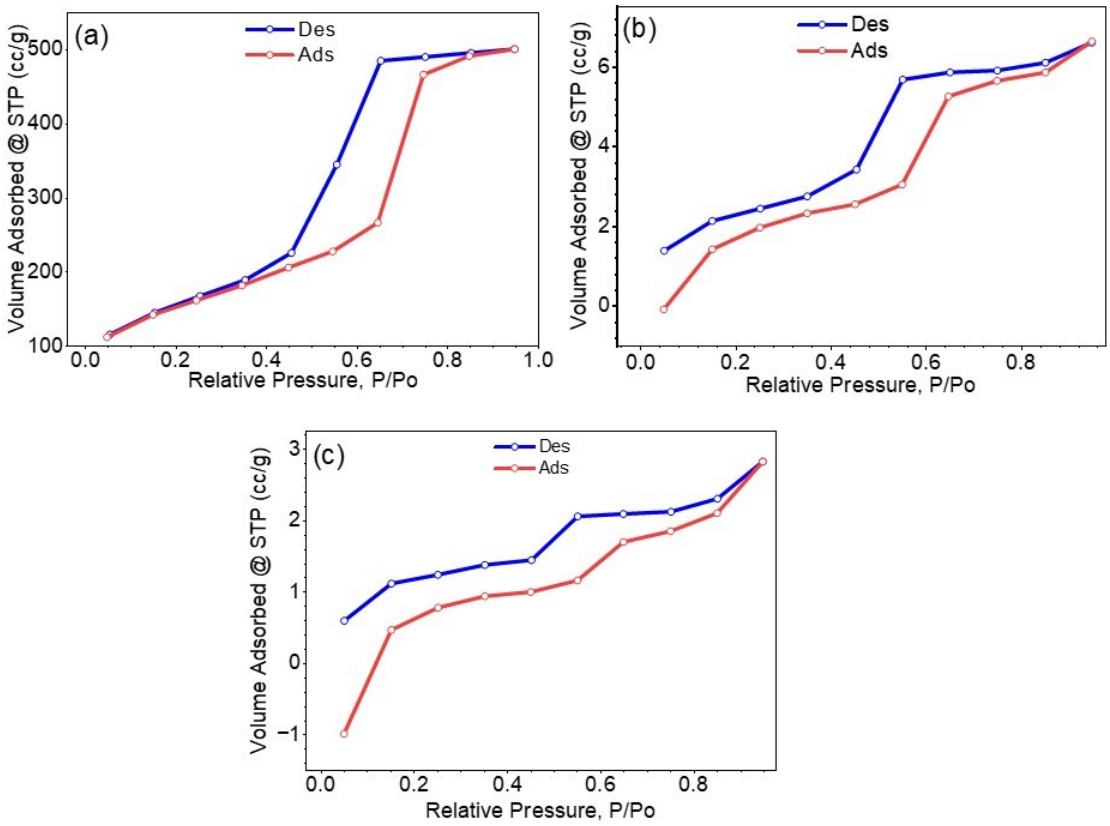

Figure 1. Isothermic Curve of (a) SBA-15, (b) Piperine-SBA15, (c) MCC-SBA15

Table 1. Pore Characterization of SBA-15, Piperine-SBA 15, and MCC-SBA 15

Parameter	SBA-15	Piperine-SBA 15	MCC-SBA 15
Surface area (m^2/g)	526.421	7.51861	3.63132
Pore volume ($\times 10^{-1}$ cm^3/g)	7.75962	0.102482	0.0438241
Pore diameter (nm)	R = 2.94807 or D = 5.89614	R = 2.72609 or D = 5.45218	R = 2.41368 or D = 4.82736

tion of the two compounds in solid form, in accordance with a previous study (Patel et al., 2020). The diffractograms of MCC:SBA-15 and piperine:SBA-15 show the same characteristics, presenting no sharp peaks and a decrease in peak intensity after adsorption into the SBA-15 mesopores. Although several small peaks are slightly higher in intensity than for pure SBA-15, the intensities are significantly lower than for pure piperine. This indicates that the adsorbed multicomponent crystal and piperine were in the amorphous phase, and adsorption was successful into the SBA-15 mesopores (Dadej et al., 2022).

DSC analysis describes thermal properties, including the glass transition, melting, and crystallization properties of a compound. The DSC thermograms of piperine, nicotinamide, and MCC (Figure 3 and Table 3) show a single and sharp endothermic peak at 131.63, 129.99, and 100.53°C, respectively, representing the substance melting points. MCC has a lower melting point, indicating a weaker lattice energy in the crystal phase, supporting the observed increase in piperine solubility and dissolution (Zaini et al., 2020b).

The DSC thermogram of SBA-15 shows a glass transition at 26.74°C and no endothermic melting peak. This supports the X-ray diffraction analysis that SBA-15 is in an amorphous state and has good thermal stability up to 150°C (Dadej et al., 2022). The DSC thermograms of MCC:SBA-15 and piperine:SBA-15 show glass transitions at 17.05 and 26.85°C, and small endothermic peaks at 115.99 and 124.12°C, respectively. These endothermic peaks likely indicate small amounts of piperine in crystal form adsorbed on the pore surface of SBA-15, incompletely incorporated into the pore structure of SBA-15 (Pardhi et al., 2017). The melting points of piperine in MCC:SBA-15 and piperine:SBA-15 are lower than for pure piperine, likely due to a decrease in crystal size as limited by the pore structure of SBA-15 (Guo et al., 2013). Another parameter related to thermal properties is enthalpy of fusion,

Table 2. Specific Peak Intensity Data of Piperine, Nicotinamide, Multicomponent Piperine-Nicotinamide, SBA 15, Multicomponent-SBA 15, and Piperine-SBA 15

2θ Position (°)	Intensity					
	Piperine	Nicotinamide	MCC	SBA 15	MCC-SBA 15	Piperine-SBA 15
12.96	1696.03	746.98	606.64	444.07	281.09	352.81
14.82	7868.25	3790.17	2363.21	310.34	339.33	350.37
15.08	648.72	6753.61	1571.63	394.77	306.44	336.68
16.04	1698.90	597.93	674.31	402.25	285.17	288.28
19.76	2841.96	1048.77	1402.62	273.74	349.95	341.02
21.39	2523.43	438.74	798.77	486.71	296.74	415.51
22.59	4813.63	884.85	1821.83	445.19	352.03	406.70
25.89	8625.05	417.50	2719.38	361.81	357.01	394.46
26.07	984.27	4851.57	739.01	336.44	275.34	234.64
27.56	444.06	5889.83	838.39	292.77	251.23	246.95

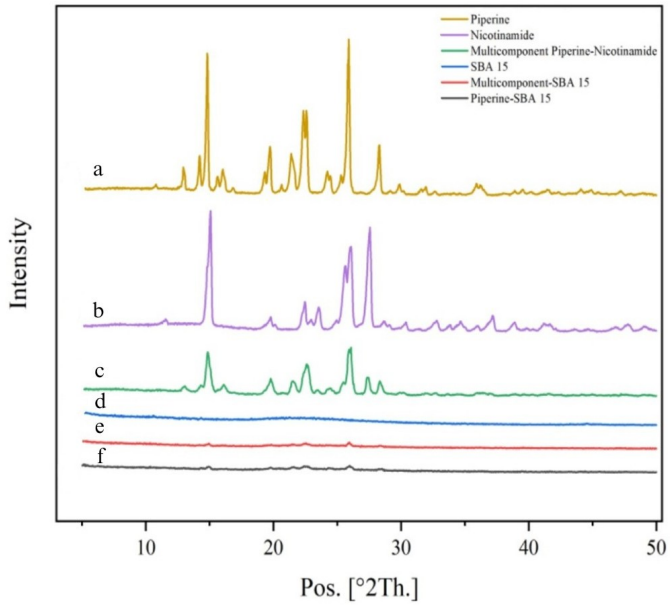

Figure 2. Diffractogram of (a) Piperine, (b) Nicotinamide, (c) Multicomponent Piperine-Nicotinamide, (d) SBA 15, (e) Multicomponent-SBA 15, (f) Piperine-SBA 15

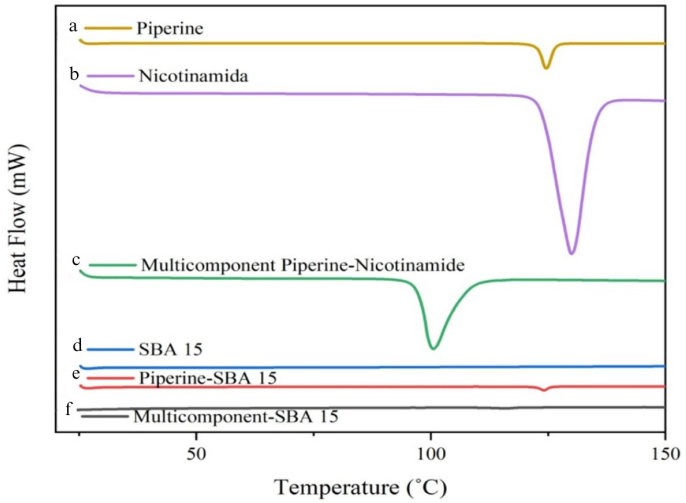

Figure 3. Thermogram of (a) Piperine, (b) Nicotinamide, (c) MCC Piperine-Nicotinamide, (d) SBA 15, (e) MCC-SBA 15,(f) Piperine-SBA 15

which describes the amount of energy required during the melting process of a substance. As seen in Table 3, the enthalpy of fusion of piperine decreases after loading into both piperine:SBA-15 and MCC:SBA-15, suggesting reduced melting energy and diminished crystallinity (Fitriani et al., 2024b). The results support the X-ray diffraction analysis.

FT-IR spectroscopic analysis is usually utilized to identify chemical bonding, determine functional groups, and confirm the presence of an adsorbate (Song et al., 2020). In this study, FT-IR spectroscopy was conducted to investigate the interaction between the adsorbate and the silica matrix, with the results shown in Figure 4.

The FT-IR spectrum of mesoporous SBA-15 shows a wide characteristic vibration band at 1055 cm^{-1} representing Si−O−Si asymmetric bending. The Si−O−Si symmetric stretching and Si-O-Si bending are described by bands at 804 and 437 cm^{-1}. A wide band at 3273 cm^{-1} represents O−H (Si−OH) and a band at 970 cm^{-1} represents external silanol (Si−OH) groups on the surface of the mesoporous silica. The band at 1663 cm^{-1} shows the water –OHgroup (H−O−H). In a study conducted by Dadej et al. (2022), the absorption bands of SBA-15 include Si−O−Si asymmetric bending at 1100-1200 cm^{-1}, Si−O−Si symmetric stretching at 800 cm^{-1} and Si−O−Si bending at 465 cm^{-1}, silanol group vibration at 960 cm^{-1}, and stretching of the –OH group of Si−OH and water molecules at 1638 and 3430 cm^{-1}, respectively (Dadej et al., 2022).

In the FT-IR spectra of piperine and nicotinamide there are differences in the range 2500-3500 cm^{-1}. For piperine, a band at 2914 cm^{-1} describes C−H stretching. Meanwhile, nicoti-

Table 3. Thermogram Data of Piperine, Nicotinamide, Multicomponent Piperine-Nicotinamide, SBA 15, Multicomponent-SBA 15, and Piperine-SBA 15

Samples	Melting Point (°C)	ΔH Fusion (J/g)
Piperine	131.63	97.20
Nicotinamide	129.99	248.68
MCC Piperine-Nicotinamide	100.53	107.60
SBA 15	-	-
MCC-SBA 15	115.99	0.66
Piperine-SBA 15	124.12	1.91

namide does not show absorption from the C−H stretch but absorption by the N−H bond is indicated by a double peak typical for primary amides at 3356 and 3146 cm^{-1}, and the C=O bond stretch at 1672 cm^{-1} indicates the amide group. The MCC sample displays N−H and a C−H stretches at the same wavenumbers as in piperine and nicotinamide, and the C=O group stretch is at 1634 cm^{-1}, close to that of nicotinamide. Furthermore, the C=C group in MCC is at the same wavenumber as in piperine at 1582 cm^{-1}, while in nicotinamide it is at 1574 cm^{-1}. Hence, there was no significant shifts between the samples, indicating no chemical interaction between piperine and nicotinamide in the multicomponent crystal (Zaini et al., 2020a).

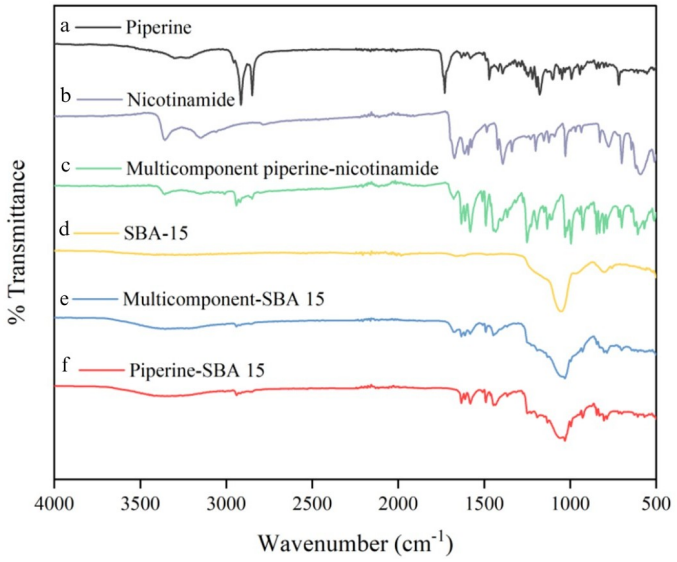

Figure 4. FTIR Spectrum of (a) Piperine, (b) Nicotinamide, (c) MCC iperine-Nicotinamide, (d) SBA 15, (e) MCC-SBA 15, (f) Piperine-SBA 15

The FT-IR spectra of MCC:SBA-15 and piperine:SBA-15 reveal absorption bands for each respective component, confirming that the MCC and piperine have been adsorbed into the pores of SBA-15. In SBA-15 loaded with MCC and piperine, the infrared absorption band at 437 cm^{-1} corresponds to T−O vibrations (transverse orientation). Additionally, the band at 1055 cm^{-1} relates to the asymmetrical Si−O−Si T−O_4 vibration, suggesting that adsorption leaves the primary structure of SBA-15 unchanged (Jangra et al., 2016). In Figure 4, it can be seen that more characteristic peaks of piperine appear in the piperine:SBA-15 spectrum than in that of MCC:SBA-15, showing that piperine is not only adsorbed in the SBA-15 channels but is also present on its surface. This result supports the results of X-ray analysis which also shows the characteristic peak of piperine in piperine:SBA-15 and MCC:SBA-15 but with an intensity lower than that of pure piperine and slightly higher than that of SBA-15.

SEM analysis is used to determine the solid sample morphology and can confirm other solid-state characterizations. The morphology of piperine (Figure 5a) shows an irregular crystal shape, while nicotinamide (Figure 5b) reveals long crystals that combine to form conglomerates. Meanwhile, the morphology of the MCC (Figure 5c) presents a slightly different shape from the piperine and nicotinamide crystals, aggregating with a smaller particle size. SEM analysis of SBA-15 (Figure 5d) shows elongated rod particles that combine to form larger structures, in accordance with the literature (Dadej et al., 2022). The morphology of MCC:SBA-15 and piperine:SBA-15 (Figures 5e and 5f, respectively), show the same morphology as pure SBA-15. These results indicate that, after adsorption, the mesoporous silica retains its original structure.

As seen in Figure 6, the distribution size of particles are in micro meter scale, in which piperine and SBA-15 show wide range particle size with average size around 100 μm which in accordance with the previous research (Sayyidina et al., 2025). The MCC of piperine -nicotinamide showed a slight decrease in particle size which was related to the grinding proses during the formation. After loading to mesoporous SBA -15, the pattern of particle distribution followed the APIs as seen in Figures 6d and 6e.

The entrapment efficiencies of piperine in piperine:SBA-15 and MCC:SBA-15 were calculated to determine the amount of active substance entrapped during the adsorption process relative to the amount added in the material synthesis, expressed as a percentage (%) (Table 4). MCC confers a higher piperine entrapment efficiency in SBA-15 (92.87%) than that of pure piperine (86.34%). A higher entrapment efficiency also reflects a higher dissolution rate. A study using azathioprine in mesoporous silica SBA-15 with an entrapment efficiency of 90.67% showed an increase in the dissolution rate of azathioprine (Jan-

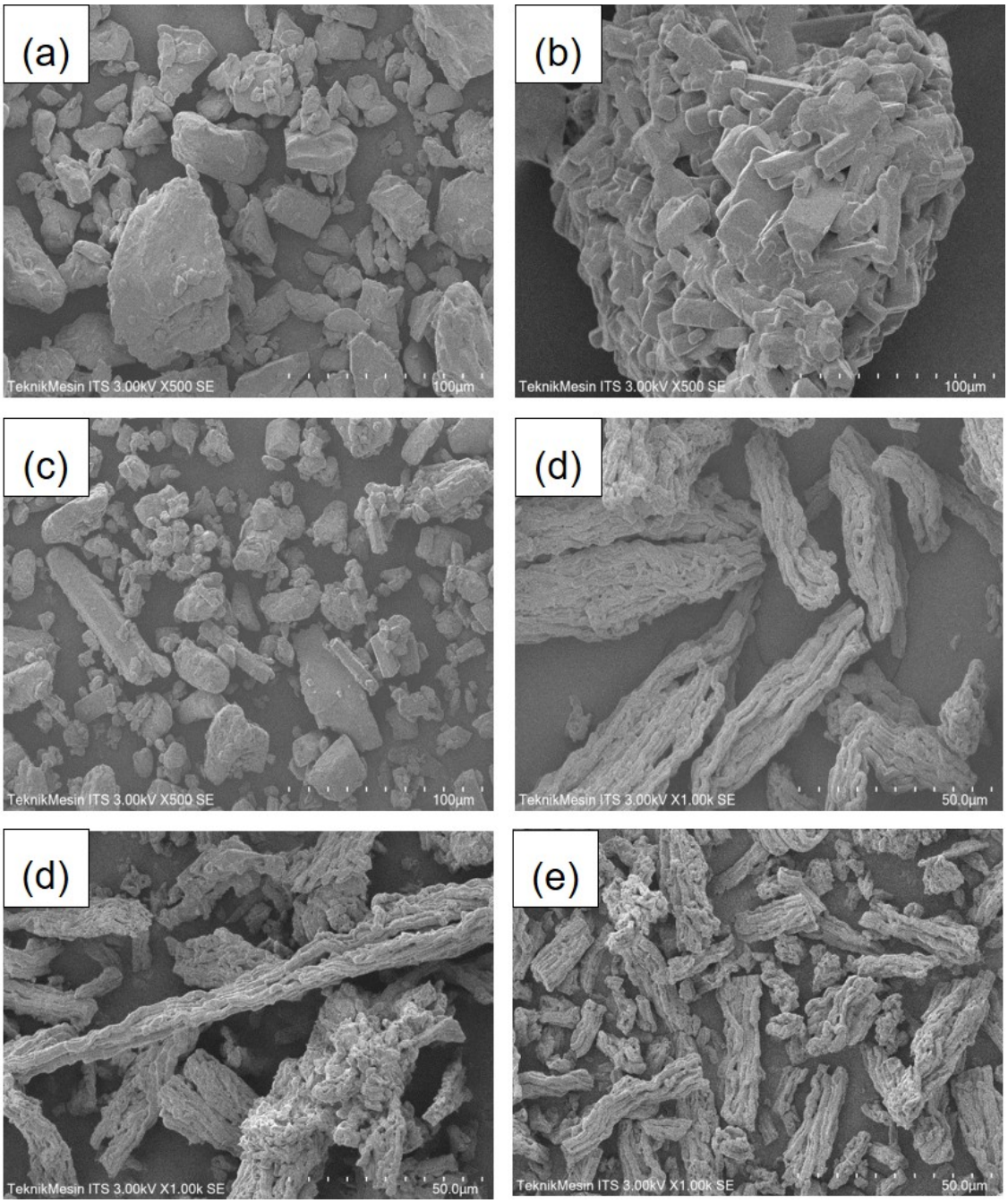

Figure 5. Morphology of (a) Piperine, (b) Nicotinamide, (c) MCC Piperine-Nicotinamide, (d) SBA 15, (e) MCC-SBA 15, (f) Piperine-SBA 15

gra et al., 2016). Another report describes an increase in the dissolution rate of valsartan with an entrapment efficiency of 59.77% in SBA-15 (Biswas, 2017). An entrapment efficiency above 60% is considered high (Supraba et al., 2021), so our results indicate high efficiency.

Solubility test results are provided in Table 5. Relative to intact piperine, piperine solubility was enhanced 1.82, 2.47, and 1.69-fold in the multicomponent crystal, MCC:SBA-15,

Table 4. Entrapment Efficiency of Drug Loaded SBA 15

Samples	% Average Entrapment Efficiency (%) (Mean ± SD)
Piperine-SBA 15	86.34 ± 0.36
MCC-SBA 15	92.87 ± 0.68

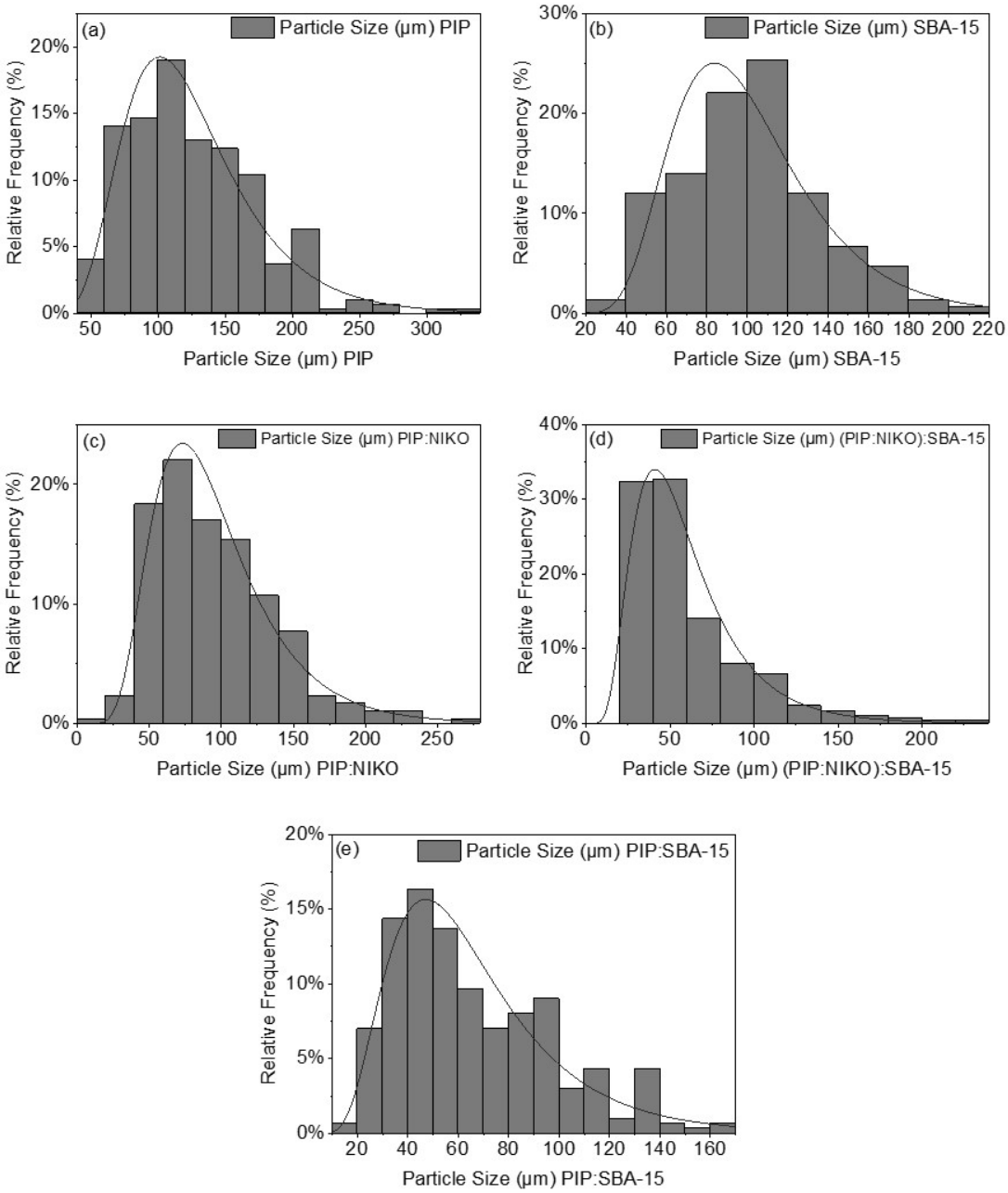

Figure 6. The Distribution Size of (a) Piperine, (b) SBA 15, (c) MCC, (d) MCC-SBA 15, (e) Piperine-SBA 15

and piperine:SBA-15, respectively. The increased solubility of piperine occurs due to its reduced degree of crystallinity after adsorption on mesoporous silica SBA-15. This is supported by DSC and PXRD analysis, which show a lower melting point and lower peak intensity than for pure piperine. A reduced melting point reflects lower lattice energy in the crystal phase, which enhances solubility and dissolution rate (Zaini et al., 2020b). In addition, the porous structure and nanometre-sized pores of the SBA-15 matrix constrain crystal growth. The amorphous phase has a reduced lattice energy requiring less energy to dissociate the components, allowing the substance to dissolve more easily (Patel et al., 2021). High solubility is also associated with a large pore volume, which increases drug wettability and drug-media interactions (Patel et al., 2021).

The dissolution rate profiles (Figure 7) show MCC:SBA-15 to have the highest average dissolution rate. Relative to pure piperine, the increase in piperine dissolution rate was 2.49, 3.07, and 2.82-fold for the multicomponent crystal, MCC:SBA-15, and piperine:SBA-15, respectively. The significant increase in dissolution rate is likely caused by retention

Table 5. Solubility Data

Samples	Solubility (mean ± SD) (mg/100 mL)	Solubility enhancement
Piperine	0.55 ± 0.17	–
MCC	1.01 ± 0.05	1.84 times
MCC-SBA 15	1.35 ± 0.02	2.47 times
Piperine-SBA 15	0.92 ± 0.02	1.69 times

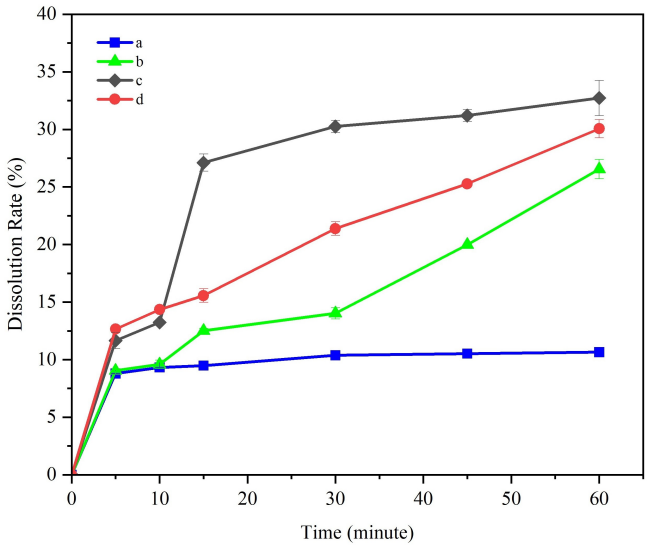

Figure 7. Dissolution Rates Profile Of (a) Piperine, (b) Multicomponent, (c) Multicomponent-SBA 15, and (d) Piperine-SBA 15

of the drug molecule in amorphous form in the pores and a decrease in the size of the piperine crystals in the pore channels (Shen et al., 2010; Guo et al., 2013). The increase in piperine dissolution rate in MCC:SBA-15 is supported by data such as a decrease in PXRD diffraction peak intensity, a decrease in melting point, and an increase in solubility.

The enhanced solubility and dissolution rate of piperine are attributed to its amorphous form generated within the pores of SBA-15. Consequently, examining the physical stability of this amorphous state during storage is essential. Physical stability studies were carried out on MCC:SBA-15 and piperine:SBA-15 samples for 2 weeks at 75, 85, and 95% RH at 40°C. An overlay of the sample diffractograms before and after the stability tests can be seen in Figures 8 and Figure 9.

In this study, the solubility of piperine after loading in SBA-15 improved significantly compared to multicomponent crystals using saccharin and succinic acid, as seen in Table 6. Piperine after adsorbed also showed less crystallinity which anticipated the further crystallization after storage which supported by the physical stability study shown the following result of XRD. This was due to the amorphization using mesoporous silica SBA-15. Regarding the nano-formulation in suspension or emulsion, it showed a slightly higher in the solubility of piperine, however the stability after storage regarding aggregation, precipitation or segregation phase need to be reconsidered.

No changes in crystallinity or phase transitions occurred at 75% and 85% RH, indicating the relative stability of piperine: SBA-15 and MCC:SBA-15 under these conditions. A stability study conducted on ibuprofen in SBA-15 at 40°C /75% RH also showed good physical stability at high relative humidity, revealed by an absence of diffraction peaks indicating recrystallization or crystal growth. Moreover, the nanometre-sized pore structure and uniform pore walls of SBA-15 maintain the drug molecules in an amorphous state, thereby preventing recrystallisation at high relative humidity (Shen et al., 2010).

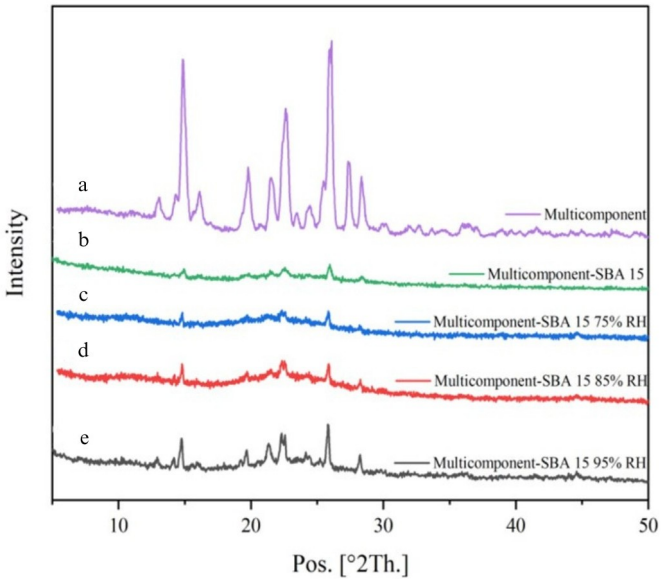

Figure 8. Diffractogram of (a) Multicomponent, (b) MCC-SBA 15, (c) MCC -SBA 15 75% RH, (d) MCC -SBA 15 85% RH, (e) MCC-SBA 15 95% RH

The diffractograms of MCC:SBA-15 and piperine:SBA-15 tested at 95% RH show a significant increase in peak intensity at 2θ 21.39°, 22.59°, and 25.89°. However, the peak intensity did not increase to the levels of the multicomponent crystal or pure piperine. This shows that the MCC and piperine on the surface of the SBA-15 pores, and not retained within the pores, cannot maintain their physical stability at high relative humidity (RH 95%), resulting in slight crystal growth. Moisture exerts a plasticizing effect on amorphous solids by increasing molecular mobility and decreasing the glass transition tem-

Table 6. The Comparison of Enhancement Solubility and Dissolution of Piperine

Method	Solubility increase	Dissolution rate increase	References
Multicomponent crystal with saccharin	–	1.82-fold	(Zaini et al., 2020b)
Multicomponent crystal with succinic acid	3.996-fold	2.185-fold	(Zaini et al., 2020a)
SNEDDS	–	3.512-fold	(Zafar et al., 2021)
Nanosuspension	–	3.65-fold	(Zafar et al., 2019)

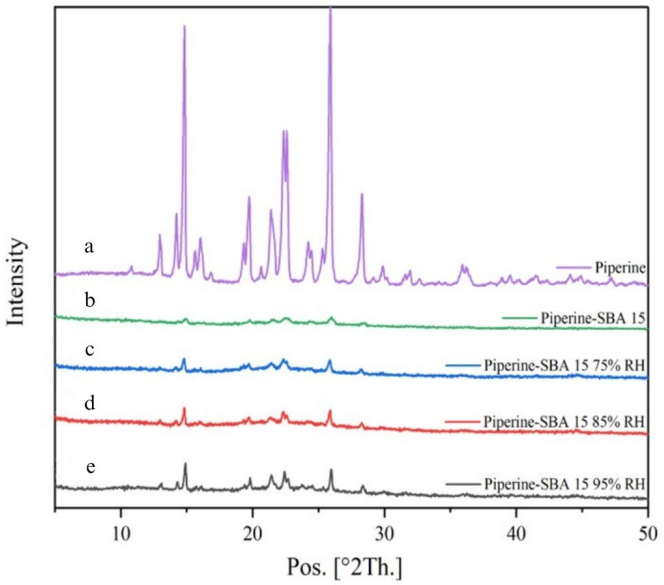

Figure 9. Diffractogram of (a) Piperine, (b)Piperine-SBA 15, (c) Piperine-SBA 15 75% RH, (d) Piperine-SBA 15 85% RH, (e) Piperine-SBA 15 95% RH

perature, thereby impacting the propensity for crystallization (Strydom et al., 2009).

4. CONCLUSIONS

The multicomponent crystal piperine/nicotinamide (MCC) was successfully loaded into the mesopores of the synthesised mesoporous silica SBA-15 carrier, as evidenced by nitrogen adsorption-desorption assays, SEM, DSC, PXRD, and FTIR. The amorphous form of MCC conferred a 2.47-fold enhancement in piperine solubility and 3.07-fold increase in piperine dissolution rate compared to pure piperine. MCC:SBA-15 can also be categorised as physically stable at 75% and 85% RH at 40°C.

5. ACKNOWLEDGMENT

The authors would like to thank Universitas Andalas for funding this research and publication under scheme PUJK 2024 (No 352/UN16.19/PT.01.03/PUJK/2024).

REFERENCES

Biswas, N. (2017). Modified Mesoporous Silica Nanoparticles for Enhancing Oral Bioavailability and Antihypertensive Activity of Poorly Water Soluble Valsartan. *European Journal of Pharmaceutical Sciences*, **99**; 152–160

Buya, A. B., A. Beloqui, P. B. Memvanga, and V. Préat (2020). Self-Nano-Emulsifying Drug-Delivery Systems: From the Development to the Current Applications and Challenges in Oral Drug Delivery. *Pharmaceutics*, **12**(12); 1194

Chakravorty, R. (2022). Nanosuspension as an Emerging Nanotechnology and Techniques for Its Development. *Research Journal of Pharmacy and Technology*, **15**(1); 489–493

Charalabidis, A., M. Sfouni, C. Bergström, and P. Macheras (2019). The Biopharmaceutics Classification System (BCS) and the Biopharmaceutics Drug Disposition Classification System (BDDCS): Beyond Guidelines. *International Journal of Pharmaceutics*, **566**; 264–281

Chaudhary, V. and S. Sharma (2017). An Overview of Ordered Mesoporous Material SBA-15: Synthesis, Functionalization and Application in Oxidation Reactions. *Journal of Porous Materials*, **24**(3); 741–749

Dadej, A., A. Woźniak-Braszak, P. Bilski, H. Piotrowska-Kempisty, M. Jóźkowiak, A. Pawełczyk, D. Dadej, D. Łażewska, and A. Jelińska (2022). Improved Solubility of Lornoxicam by Inclusion into SBA-15: Comparison of Loading Methods. *European Journal of Pharmaceutical Sciences*, **171**; 106133

Fitriani, L., H. Azizah, U. Hasanah, and E. Zaini (2022). Enhancement of Curcumin Solubility and Dissolution by Adsorption in Mesoporous SBA-15. *International Journal of Applied Pharmaceutics*, **15**(1); 61–67

Fitriani, L., C. M. Azzahra, A. Jessica, U. Hasanah, and E. Zaini (2024a). Improvement of Solubility Usnic Acid Loaded on Mesoporous Silica SBA-15 and Physicochemical Characterization. *Science and Technology Indonesia*, **9**(2); 251–259

Fitriani, L., S. Tirtania, S. Umar, and E. Zaini (2024b). Enhancing the Solubility and Dissolution Rate of Piperine via Preparation of Piperine–Hydroxypropyl Methylcellulose 2910 Solid Dispersion System Using Freeze-Drying Method. *Journal of Pharmacy & Pharmacognosy Research*, **12**(1); 175–183

Guo, Z., X. M. Liu, L. Ma, J. Li, H. Zhang, Y. P. Gao, and Y. Yuan (2013). Effects of Particle Morphology, Pore Size and Surface Coating of Mesoporous Silica on Naproxen Dis-

solution Rate Enhancement. *Colloids and Surfaces B: Biointerfaces*, **101**; 228–235

Haq, I., M. Imran, M. Nadeem, T. Tufail, T. A. Gondal, and M. S. Mubarak (2021). Piperine: A Review of Its Biological Effects. *Phytotherapy Research*, **35**(2); 680–700

Hasanah, U., F. Rizky, M. C. I. Mohd Amin, and E. Zaini (2025). Ticagrelor Solubility and Dissolution Rate Enhancement Using Mesoporous Silica SBA-15. *Science and Technology Indonesia*, **10**(2); 598–604

Jangra, S., P. Girotra, V. Chhokar, and V. K. Tomer (2016). In-Vitro Drug Release Kinetics Studies of Mesoporous SBA-15–Azathioprine Composite. *Journal of Porous Materials*, **23**; 679–688

Jaramillo, L. Y., W. Henao, and M. Romero-Sáez (2020). Synthesis and Characterization of MCM-41–SBA-15 Mixed-Phase Silica with Trimodal Mesoporous System and Thick Pore Wall. *Journal of Porous Materials*, **27**(6); 1669–1676

Júnior, J. V. C., J. A. B. Dos Santos, T. B. Lins, R. S. de Araújo Batista, S. A. de Lima Neto, A. de Santana Oliveira, F. H. A. Nogueira, A. P. B. Gomes, D. P. de Sousa, and F. S. de Souza (2020). A New Ferulic Acid–Nicotinamide Cocrystal with Improved Solubility and Dissolution Performance. *Journal of Pharmaceutical Sciences*, **109**(3); 1330–1337

Kusumorini, N., A. K. Nugroho, S. Pramono, and R. Martien (2022). Spray-Dried Self-Nanoemulsifying Drug Delivery Systems as Carriers for the Oral Delivery of Piperine: Characterization and In Vitro Evaluation. *Journal of Applied Pharmaceutical Science*, **12**(9); 43–57

Lutfiyah, D. S., L. Fitriani, M. Taher, and E. Zaini (2022). Crystal Engineering Approach in Physicochemical Properties Modifications of Phytochemical. *Science and Technology Indonesia*, **7**(3); 353–371

Nair, A. R., Y. D. Lakshman, V. S. K. Anand, K. S. N. Sree, K. Bhat, and S. J. Dengale (2020). Overview of Extensively Employed Polymeric Carriers in Solid Dispersion Technology. *AAPS PharmSciTech*, **21**; 1–20

Octavia, M. D., H. Hasmiwati, G. Revilla, and E. Zaini (2023). Multicomponent Crystals of Piperine-Nicotinic Acid: The Physicochemical and Dissolution Rate Properties. *Tropical Journal of Natural Product Research*, **7**(8); 3701–3705

Pardhi, V., R. B. Chavan, R. Thipparaboina, S. Thatikonda, V. G. M. Naidu, and N. R. Shastri (2017). Preparation, Characterization, and Cytotoxicity Studies of Niclosamide Loaded Mesoporous Drug Delivery Systems. *International Journal of Pharmaceutics*, **528**(1–2); 202–214

Patel, R. D., M. K. Raval, T. M. Pethani, and N. R. Sheth (2020). Influence of Eutectic Mixture as a Multi-Component System in the Improvement of Physicomechanical and Pharmacokinetic Properties of Diacerein. *Advanced Powder Technology*, **31**(4); 1441–1456

Patel, R. J., A. A. Patel, and H. P. Patel (2021). Stabilized Amorphous State of Riluzole by Immersion-Rotavapor Method With Synthesized Mesoporous SBA-15 Carrier to Augment In-Vitro Dissolution. *Journal of Drug Delivery Science and Technology*, **61**; 102270

Quilaqueo, M., S. Millao, I. Luzardo-Ocampo, R. Campos-Vega, F. Acevedo, C. Shene, and M. Rubilar (2019). Inclusion of Piperine in β-Cyclodextrin Complexes Improves Their Bioaccessibility and In Vitro Antioxidant Capacity. *Food Hydrocolloids*, (91); 143–152.

Sayyidina, F., A. Gumala, E. Zaini, D. Hanifa, and U. Hasanah (2025). Amine-Functionalized Mesoporous Silica SBA-15 for Enhanced Solubility and Release Rate of Gliclazide. *Science and Technology Indonesia*, **10**(3); 963–971

Shen, S., W. A. I. K. Ng, L. Chia, Y. Dong, and R. B. H. Tan (2010). Stabilized Amorphous State of Ibuprofen by Co-Spray Drying With Mesoporous SBA-15 to Enhance Dissolution Properties. *Journal of Pharmaceutical Sciences*, **99**(4); 1997–2007

Song, Y., Y. Cong, B. Wang, and N. Zhang (2020). Applications of Fourier Transform Infrared Spectroscopy to Pharmaceutical Preparations. *Expert Opinion on Drug Delivery*, **17**(4); 551–571

Springuel-Huet, M.-A., J.-L. Bonardet, A. Gédéon, Y. Yue, V. N. Romannikov, and J. Fraissard (2001). Mechanical Properties of Mesoporous Silicas and Alumina–Silicas MCM-41 and SBA-15 Studied by N2 Adsorption and 129Xe NMR. *Microporous and Mesoporous Materials*, **44–45**; 775–784

Strydom, S., W. Liebenberg, L. Yu, and M. de Villiers (2009). The Effect of Temperature and Moisture on the Amorphous-to-Crystalline Transformation of Stavudine. *International Journal of Pharmaceutics*, **379**(1–2); 72–81

Supraba, W., J. Yuliantoni, and A. Dwi (2021). The Effect of Stirring Speeds to the Entrapment Efficiency in a Nanoparticles Formulation of Java Plum's Seed Ethanol Extract (Syzygium Cumini). *Acta Chim. Asiana*, **4**(1); 197–202

Thahir, R., A. W. Wahab, N. L. Nafie, and I. Raya (2019). Synthesis of High Surface Area Mesoporous Silica SBA-15 by Adjusting Hydrothermal Treatment Time and the Amount of Polyvinyl Alcohol. *Open Chemistry*, **17**(1); 963–971

Thommes, M. and K. A. Cychosz (2014). Physical Adsorption Characterization of Nanoporous Materials: Progress and Challenges. *Adsorption*, **20**(2); 233–250

Van Der Meer, J., I. Bardez-Giboire, C. Mercier, B. Revel, A. Davidson, and R. Denoyel (2010). Mechanism of Metal Oxide Nanoparticle Loading in SBA-15 by the Double Solvent Technique. *Journal of Physical Chemistry C*, **114**(8); 3507–3515

Wdowiak, K., R. Pietrzak, E. Tykarska, and J. Cielecka-Piontek (2023). Hot-Melt Extrusion as an Effective Technique for Obtaining an Amorphous System of Curcumin and Piperine with Improved Properties Essential for Their Better Biological Activities. *Molecules*, **28**(9); 3848

Yadav, D., J. Savjani, K. Savjani, A. Kumar, and S. Patel (2022). Pharmaceutical Co-Crystal of Antiviral Agent Efavirenz with Nicotinamide for the Enhancement of Solubility, Physicochemical Stability, and Oral Bioavailability. *AAPS Pharm-*

SciTech, **24**(1); 7

Zafar, A., S. S. Imam, N. K. Alruwaili, O. A. Alsaidan, M. H. Elkomy, M. M. Ghoneim, S. Alshehri, A. M. A. Ali, K. S. Alharbi, and M. Yasir (2021). Development of Piperine-Loaded Solid Self-Nanoemulsifying Drug Delivery System: Optimization, In-Vitro, Ex-Vivo, and In-Vivo Evaluation. *Nanomaterials*, **11**(11); 2920

Zafar, F., N. Jahan, Khalil-Ur-Rahman, and H. N. Bhatti (2019). Increased Oral Bioavailability of Piperine from an Optimized Piper Nigrum Nanosuspension. *Planta Medica*, **85**(3); 249–257

Zaini, E., A. Afriyani, L. Fitriani, F. Ismed, A. Horikawa, and H. Uekusa (2020a). Improved Solubility and Dissolution Rates in Novel Multicomponent Crystals of Piperine with Succinic Acid. *Scientia Pharmaceutica*, **88**(2); 21

Zaini, E., L. Fitriani, R. Y. Sari, H. Rosaini, A. Horikawa, and H. Uekusa (2019). Multicomponent Crystal of Mefenamic Acid and N-Methyl-D-Glucamine: Crystal Structures and Dissolution Study. *Journal of Pharmaceutical Sciences*, **108**(7); 2341–2348

Zaini, E., R. P. Marhammah, L. Fitriani, U. Hasanah, and S. Umar (2021). The Preparation and Characterization of the Solid Dispersion of Piperine with Hydroxypropyl Methylcellulose (HPMC) 2910 Using Spray Drying. *Tropical Journal of Natural Product Research (TJNPR)*, **5**(12); 2103–2107

Zaini, E., D. Riska, M. D. Oktavia, F. Ismed, and L. Fitriani (2020b). Improving Dissolution Rate of Piperine by Multicomponent Crystal Formation with Saccharin. *Research Journal of Pharmacy and Technology*, **13**(4); 1928–1932

